A FIRST EVALUATION OF THE FEA

Aldo Buccafurni, Andrea Orazi
ANPA, National Agency for the Environment Protection
Rome,
Italy

Abstract

An EA core model suitable for MCNP code has been built on the available reference data and engineering judgment, in case of lack of information. The EA was modelled in cylindrical geometry by subdividing the actual EA structure into five regions: target, buffer, inner core, outer core, breeder.

ORIGEN calculations were carried out for the core region at a specific power of 52.8 MW/t; for the breeder region a total flux value of 5.49×10^{14} $n.cm^{-2}.s^{-1}$, obtained from MCNP calculations, was used. The calculations were carried out using the LMFBR libraries available in order to select the best performing one comparing the results to the data available.

Calculations were performed to verify the nominal effective multiplication factor as well as the thermal power and neutron flux at BOL conditions for each region and whole systems.

General description

The first version of Rubbia's Energy Amplifier (EA) [1] was an Accelerator Driven System (ADS) in which the subcritical reactor was a Thorium fuelled PWR-like core. In the reactor side of the EA concept, that is the one considered in the present work, the evolution of the design moved from a thermal to a lead cooled fast concept maintaining the Th mixed oxides fuel. The physical basis and the conceptual design of the Fast Energy Amplifier (FEA) are illustrated in Reference 2, that was the main source of information used in the present work.

The general layout [2,3] can be grouped into three main components: the accelerator, the heat generating unit, the heat dissipation or utilisation devices. Their description can be found in the quoted references.

Model development

The main goals of the calculations were to verify the completeness and consistency of the data available and to set up base decks and models suitable to be used as reference for further calculations and verifications.

A preliminary EA three dimensional simulation was carried out using MCNP [4] version 4.2 Monte Carlo computer code. The EA was modelled in cylindrical geometry by subdividing the actual EA structure into three main regions: the target/source region, the core, the vessel and internals; the model was built on the available reference data [2,5,6] and engineering judgment, in case of lack of information.

Target/source region

The target and buffer have an external radius [2] of 40 cm. The target/source region, of 20 cm in diameter and 1.2 m in high, was modelled (Figure 1) with cylindrical meshes according to a previous calculation [7] performed with LAHET [8] code.

The MCNP neutron source distribution is derived from LAHET calculation performed with proton energy of 1 GeV and neutron energy cut-off of 20 MeV. These calculations showed an almost isotropic angular distribution and substantial spatial independence of the energy spectra. The neutron source was described in terms of volumetric distributions in the target meshes and energy spectrum for whole target.

Figure 1. **Target/source zone meshes**

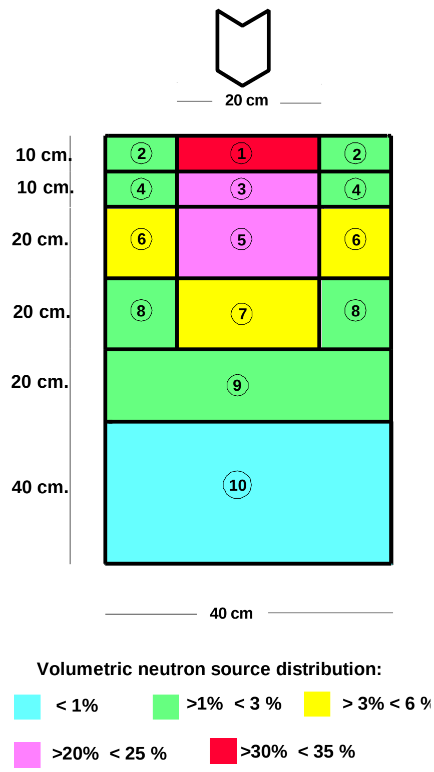

Core

Core is made of hexagonal fuel assemblies similar to fast reactor ones. The EA core is divided into three regions:

1) An innermost ring with a larger pitch between pins to flat the power distribution, using pellets of ThO_2 enriched with 10% by weight of $^{233}UO_2$.
2) A middle annulus filled with fuel assemblies of ThO_2 enriched with 10% by weight of $^{233}UO_2$.
3) An outermost ring of breeder assemblies with pellets of ThO_2.

The main parameters of the EA core are summarised in Table 1. As the number of fuel assemblies in the inner and outer core zone are not available, they have been estimated from the pin volume, the total fuel mass and the power density. The solution leads to 14 and 106 fuel assemblies for the inner and outer core zone respectively.

Table 1. **Main design parameter of FEA core**

Fuel pellet inner diameter	1.1 mm
Fuel pellet outer diameter	7.3 mm
Gap thickness	0.1 mm
Fuel clad thickness	0.35 mm
Fuel active length	150 cm
Fuel bundle inner apothem	113 mm
Fuel bundle thickness	3 mm
Flat to flat of fuel assembly module	234 mm
Clad length above/below active zone	90 cm (each side)
Clad outer diameter above/below active zone	5.0 cm
Fuel bundle total length	5.3 m
Number of fuel bundles in the inner and outer core zone	120
Number of fuel bundles in the breeder zone	42
Number of fuel pins of inner core fuel assemblies	331
Number of fuel pins of outer core and breeder fuel assemblies	397
Total thermal power	1 500 MW
Specific power (power density by oxide mass)	52.8 W/g
Power density	523 W/cm^3
Initial fuel mass (ThO_2 + 0.1 $^{233}U_{O2}$)	28.41 ton
Initial breeder mass (ThO_2)	5.6 ton

The fuel elements were arranged in hexagonal geometry. While breeder zone has exactly 42 elements, the inner one has only 12 out of 14 fuel elements needed to fill the inner core zone. This geometrical inconsistency, due to the lack of detailed core description, is overcome, by the assumption of cylindrical geometry for the MCNP model (Figure 2).

The flat to flat length of fuel assembly module was assumed as thickness of the inner core and breeder regions. The core region was divided into five axial zones with constant cross sections:

1) Active length [2] (1.5 m).
2) Fuel pins zone above and below the active length (0.9 m each): pins have an upper and lower plenum to ensure the required burn-up, but with a smaller diameter to reduce the pressure drop through the core.

Fuel bundle zone above and below fuel pins (1 m each).

The main geometrical parameters of MCNP core model are summarised in Figure 2; minimum required areas are calculated from actual dimension of the EA fuel assemblies to verify the spatial consistency of the assumptions. For each core zone, the cross sections filled with fuel, structural material and coolant are calculated from the actual geometrical data of the EA fuel assembly module.

The fuel mass was divided into the different core regions by weighting with the inner and outer core volume filled with fuel while the structural material (low absorption steel: HT-9) and coolant (lead) mass was calculated using the material density at their operative temperature.

Figure 2. **MCNP model of EA core**

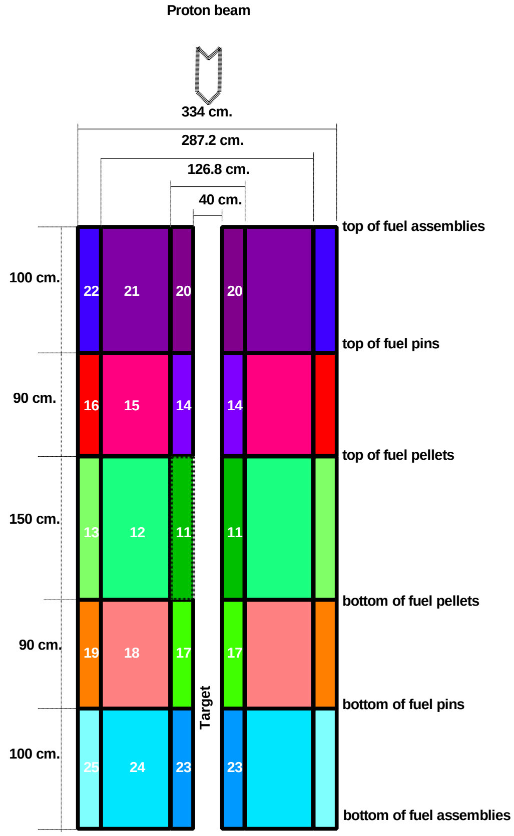

Vessel and internals

The main design parameters of EA vessel and internals are listed on Table 2. An overall view of the EA MCNP model is provided by Figure 3.

Figure 3. **MCNP model of EA vessel and internals**

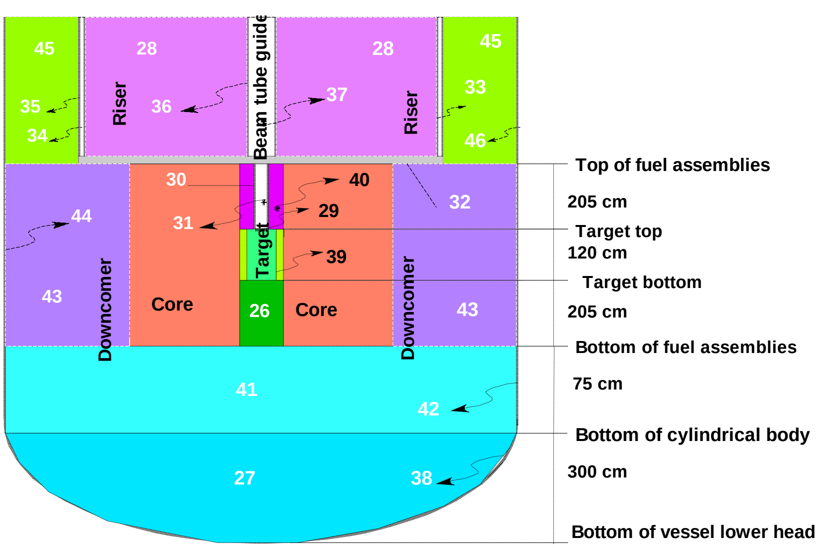

Table 2. **Main design parameter of EA vessel and internals**

Vessel outer diameter = 6 m.
Vessel thickness = 7 cm.
Vessel with an hemispherical lower head.
Beam pipe external diameter = 30 cm.
Beam pipe external diameter in the core zone = 20 cm.
Beam pipe thickness = 3 mm.
Beam window thickness = 3 mm at edges and 1.5 mm at centre (hemispherical shape).
Riser external diameter = 3.65 m.
Riser thickness = 3 cm (double wall with vacuum between, each region are 1 cm thick).
Core support disk thickness = 15 cm.

The model extends to 25 m in height and 6 m in diameter and includes:

- The vessel wall.
- The downcomer near the riser and the core.
- The vessel lower head.
- The core.
- The target and the central buffer region.
- The beam tube guide walls and internal voided region in the riser and core zone.
- The beam window, modelled as a disk with the average thickness.
- The core support structure has been modelled as a disk 15 cm thick, made of 60% of steel, the remaining 40% being holes for various purposes.
- The cylindrical double wall barrel with vacuum between, which separates the riser from downcomer.

Though the model could seem excessively detailed from the point of view of criticality and flux calculation, it will save a lot of work for the future simulations of the system.

Irradiation model

The main data requested for ORIGEN [9] calculations are power history and material compositions. Concerning the power history, a 5 year (1 825 days) full power operation is used [2]. For the core region, a power irradiation was used at a specific power of 52.8 MW/t; for the breeder region, a flux irradiation was used with a total flux value of 5.49×10^{14} n/(cm² s) obtained from the MCNP calculations. For the material composition, the same core description of the Monte Carlo model is used to quantify the number of fuel assemblies in the inner and outer core.

EA steady state results at BOL

As a first step, some calculations were performed to verify the nominal effective multiplication factor as well as the thermal power and neutron flux at Begin Of Life (BOL) conditions.

In order to achieve the steady state value of the effective multiplication factor (k_{eff} = 0.98) [2] several calculations were performed by varying the enrichment in $^{233}U_{92}$ of the fuel loaded in the core at BOL. The results lead to a fuel enrichment of 10.33% which corresponds to the nominal EA multiplication factor. The fuel composition was selected for the subsequent power and flux calculations.

Table 3 lists the results for the flux and power calculations for each region and whole systems.

The energy released per fission in ^{233}U calculated by MCNP code is 180.84 MeV while, considering all contributions to the recoverable energy (kinetic energy of fission fragments and fission neutrons, β and γ rays from fission product decay, prompt γ rays and γ rays from capture of structural material) we have an energy ranging from 194 to 203 MeV/fission (depending upon the structural material in the reactor) [13].

Taking into account the above considerations and the beam heat depositions in lead and window (7.07 MW) [2], the total FEA power is estimated to range from 1 347 to 1 409 MWth which is in reasonable agreement with the nominal power of 1 500 MW_{th}. The standard deviation of the Monte Carlo calculations is 6.18% (from 83 to 87 MW) and many uncertainties already exists for the spallation neutron yield.

Table 3. **Fast energy amplifier steady-state calculation at BOL**

Region	**Neutron flux [n/(cm^2 s)]**	**Flux s (%)**	**Fission prompt power (MW)**	**Fission power s (%)**
Inner Core	3.42049×10^{15}	2.44	201.08	3.51
Outer Core	2.03134×10^{15}	2.87	1,047.10	4.08
Inner and outer core average	2.20805×10^{15}	3.77		
Breeder	5.63569×10^{14}	2.98	0.60	3.03
Core and breeder average	1.75340×10^{15}	2.80	1,248.78	6.18

System effective multiplication factor (K_{eff}) = 0.980022 (σ = 0.060 %).
Spallation neutron yield = 26.5.
Proton beam nominal current = 12.5 mA.

As regards the neutron flux, a direct comparison is not possible because its value is not explicitly indicated in the FEA nominal parameters of chapter 4 of Reference 2. On the other hand, there is a reasonable confidence that the calculated value is in good agreement with the FEA ones; in fact, Table 2.3 of chapter 2 in Reference 2 reports a neutron flux of 2.33 x 10^{15} n/(cm² s) for a power density of 60 W/g_{Th} at breeding equilibrium while the calculated (averaged inner and outer core) MCNP value is of 2.21 x 10^{15} for a power density of 52.8 W/g_{MOX} at BOL.

Irradiation calculations

For the core region (inner and outer), the calculations were carried out considering a core power of 1 500 MW with a specific power of 52.8 W/g of oxide for a 5 year cycle (1 825 Effective Full Power Days, EFPD). These data lead to a total mass of 28.409 t of oxide and to a burn-up of 96 GWd/t compared to 28.41 t and 100 GWd/t of Reference 2. Using the cross section values for ^{232}Th and ^{233}U, a flux value of about 2.6×10^{15} n/(cm^2 s) was estimated compared to an average neutron flux value from ORIGEN ranging from about 2.43×10^{15} n/(cm^2 s) to 2.49×10^{15} n/(cm^2 s) according to the used library (from 2.52×10^{15} n/(cm^2 s) to 2.56×10^{15} n/(cm^2 s) in the first time step of 3 days) and of about 2.21×10^{15} n/(cm^2 s) from the MCNP at BOL.

Figure 4 shows the obtained k_∞ values during the cycle. The previous values are normalised to 0.98 at BOL. It is very difficult to compare these results because we cannot find a figure with data such as to be qualitatively compared. The only comment we can make at the moment is that our values seem to be higher. As concerns the ORIGEN libraries used, the qualitative responses are similar, except for the N15 advanced oxide recycle one. That gives a weight of the neutron absorption in the core region higher by a factor of greater than two, compared to the results of the other two libraries.

In the following Figures 5 and 6 the mass ratio between ^{233}U and ^{232}Th and between ^{233}Pa and ^{233}U are represented respectively. As concerns the mass ratio, all the libraries give values very close to each other.

In order to compare correctly the numerical values in Figure 5 with those in the corresponding Figure 5.5 of Reference 2, we have to multiply the values by 0.9957, that is the ratio of the atomic masses of Th and ^{233}U. We first notice that the initial value at 0 burn-up is different; that means that we are starting from initial conditions that are different and that there is no full consistency among the data of Reference 2. Anyway some qualitative comparison can be done. We have about the same decrease in weight ratio of 0.001 at about the same time 5 GWd/t, but we have a relative higher ^{233}U build-up leading to a value of about 0.13 compared to about 0.116 at the same burn-up.

Figure 4. **ORIGEN II k¥ values normalised to 0.98 at BOL**

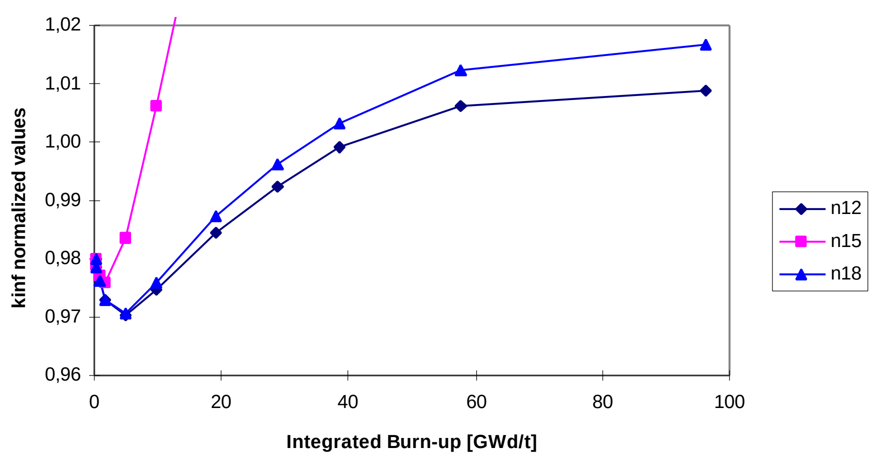

Figure 5. **Mass ratio between ^{233}U and ^{232}Th along irradiation in the inner and outer core**

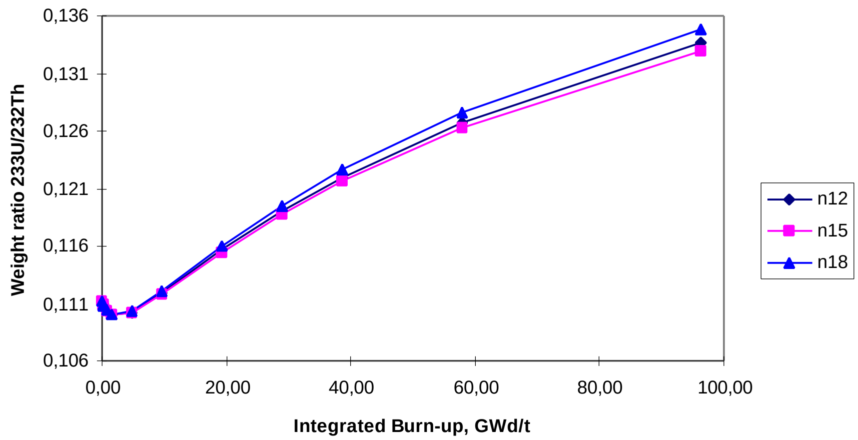

Figure 6. **Mass ratio between ^{233}Pa and ^{233}U along irradiation in the inner and outer core**

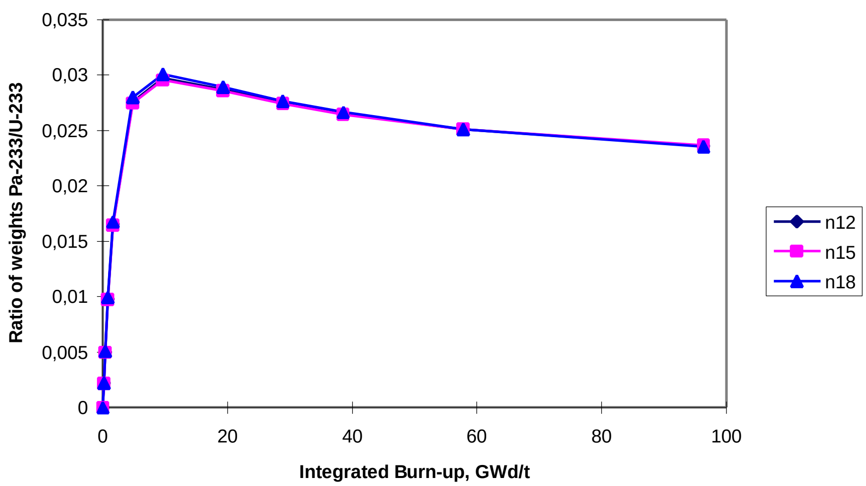

As concerns the ^{233}Pa and ^{233}U ratio we obtain a higher value of about 0.03 at 10 GWd/t and a value of 0.024 at 96 GWd/t compared to the maximum value of 0.026 at about 12 GWd/t and 0.024 at 96 GWd/t. The results show a higher maximum value at the same burn-up and in the flat region the results of Reference [2] seem linear.

The results obtained, for the breeder region, from the two libraries used are the same for all the parameters analyzed.

Concerning the specific power, in Figure 7, we get at end of cycle a value of 29.6 MW that corresponds to about 5.3 W/g to be compared to 3.0 W/g of Reference 2. For the ^{233}U amount, in Figure 8, we produced 226.5 kg compared to 242.7 kg of Table 4.1 in Reference 2, but there is no evidence that the two values refer to the same period.

Figure 7. **Breeder region: specific power behaviour**

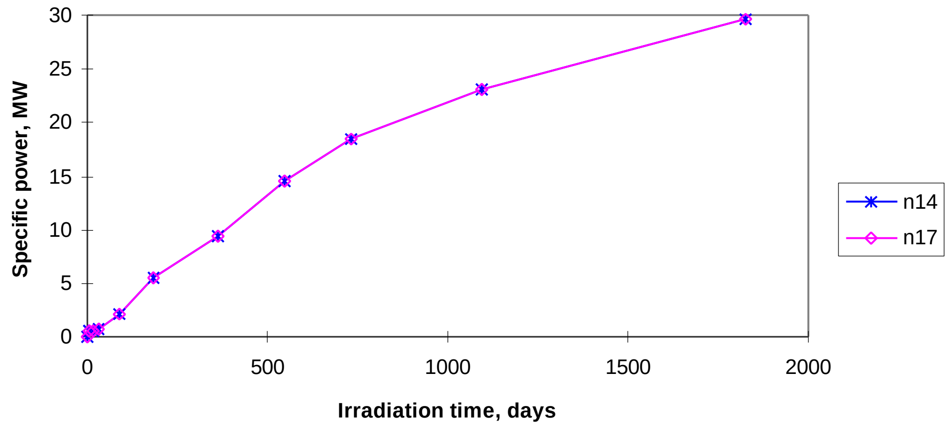

Figure 8. **Breeder region: concentration evolution of the actinides with the larger mass inventory at end of cycle**

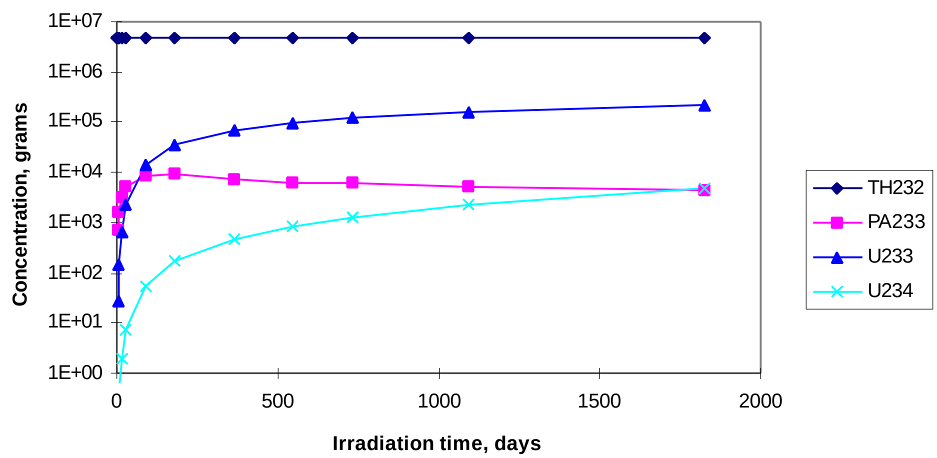

Preliminary conclusions

This analysis represents only the first step of a conceptual safety analysis of Rubbia's FEA which should follow the steps listed below:

1) Evaluate, at BOL, the steady state multiplication factor, thermal power and neutron flux.
2) Perform several burn-up calculations in order to estimate the k_{eff} evolution and the system effectiveness in reducing the final waste inventory (burning performances).
3) To evaluate the plant behaviour under transient and accident conditions.

The ORIGEN or CINDER code coupled with LAHET and MCNP can, in principle, perform the calculations of point 2 but it will require a lot of computer time as well as calculation and typing work to interface the codes. The optimal solution is represented by the integrated code MCNPX (in development at LANL) which should be able to simulate the spallation process, the neutron transport and interaction (with Monte Carlo method) and the burn-up evolution.

For the simulation of the system (point 3), some work need to be done in order to develop a set of equations able to describe the power evolution during the transients/accidents and the simple point kinetic model based on reactivity coefficient seems to be no longer applicable: a system fed by a consistent source will not behave by following essentially the main harmonic because the source also excites the superior flux modes.

In general it can be said that the system concept does not have the chance to be less complex than the fast reactor, in terms of protection and control systems; in fact, though the system is subcritical, the following aspect plays a negative role in terms of safety and system simplification:

- Several critical masses are still present in the core: some core geometrical deformations could lead to a critical configuration.
- In case of fuel cladding failure the pellets will float on the liquid lead.
- The local power evolution during accidents and transients need to be deeply investigated: though in case of complete loss of coolant (lead) our previous calculation [11] indicates a decrease of the multiplication factor mainly due to the major influence of the (n, 2n) lead reactions in respect to the parasitic absorption and some local lead vaporisation (local void coefficient) could lead to a local power increase.

Finally, it should be noted that the choice of an operative multiplication factor so close to the unit (0.98) permits to achieve an acceptable thermal power with a relatively low proton beam current but it raises some safety concerns. The above considerations suggest that the k_{eff} evolution during the burn-up over the whole reactor life should be carefully evaluated, being a possible critical (both in sense of dangerous and neutronic) aspect from the safety margin point of view.

REFERENCES

[1] F. Carminati *et al*, *An Energy Amplifier for Cleaner and Inexhaustible Nuclear Energy Production Driven by a Particle Beam Accelerator*, CERN/AT/93-45 (ET), Geneva, 1 November (1993).

[2] C. Rubbia *et al.*, *Conceptual Design of a Fast Neutron Operated High Power Energy Amplifier*, CERN/AT/95-44 (ET), Geneva, 29 September (1995).

[3] C. Rubbia, J.A. Rubio, *A Tentative Programme Towards a Full Scale Energy Amplifier*, CERN/LHC/96-11 (EET), Geneva, 15 July (1996).

[4] R. A. Foster *et al.*, *MCNP – A General Monte Carlo for Neutron and Photon Transport Manual*, Los Alamos National Laboratory, Briesmester Editor.

[5] R, Fernandez *et al*, *A Preliminary Estimate of the Economic Impact of the Energy Amplifier*, CERN/LHC/96-01 (EET), 18 February (1996).

[6] C. Rubbia, *A Comparison of the Safety and Environmental Advantages of the Energy Amplifier and Magnetic Confinement Fusion*, CERN/AT/95-58 (ET). 29 December (1995).

[7] A. Buccafurni, A. Orazi *et al.*, *Three-Dimensional Analysis of the Los Alamos Accelerator Driven Transmutation System* – (third part), Energia Nucleare, anno 12 n. 3. September – December (1995).

[8] R.E. Prael, H. Lichtenstein, *User Guide to LCS: The LAHET Code System*, LANL, LA-UR-89-3014, September (1989).

[9] A.G. Croff, *A User's Manual for the ORIGEN2 Computer Code*, ORNL/TM-7175, July (1980).

[10] John R. Lamarsh, *Introduction to Nuclear Reactor Theory*, (New York University) Addison-Wesley Publishing Company, (1972).

[11] A. Orazi, A. Buccafurni, *Commenti all'ipotesi di Rubbia per il sistema di produzione di* H_2, ANPA Internal Note, (1995).